J Supercond Nov Magn
DOI 10.1007/s10948-016-3585-0

ORIGINAL PAPER

Role of Coupling Divalent and Tetravalent Metal Ions on the Elastic and Electric Properties of $CoFe_2O_4$ Ferrites Prepared by Sol–Gel Method

S. S. Desai[1] · R. A. Pawar[2] · S. S. Jadhav[3] · Sagar E. Shirsath[4] · S. M. Patange[1]

Received: 8 April 2016 / Accepted: 7 June 2016

Abstract The effect of Zn–Ti substitution on the infrared spectroscopy, elastic, dielectric, and resistivity properties of $CoZn_xTi_xFe_{2-2x}O_4$ ferrites (where x = 0.0–0.4 in steps of 0.1) is investigated in the paper. All the samples were synthesized by the sol–gel method. Infrared spectroscopy shows two major absorption bands indicating that the prepared samples are in spinel structure. Elastic properties and dielectric properties are measured at room temperature and Zn–Ti is substitution dependent. The dc resistivity is measured using a two-probe method in the temperature range 300 to 650 K. The dielectric constant decreased whereas dc resistivity increased with the Zn–Ti substitution. The elastic constant decreases with increases in Zn–Ti ions.

Keywords Ferrite nanoparticles · Infrared spectroscopy · Elastic properties · Dielectric properties

✉ S. M. Patange
smpatange@rediffmail.com

[1] Materials Research Laboratory, Shrikrishna Mahavidyalaya, Gunjoti, MS 413613 India

[2] Department of Physics, Arts, Commerce and Science College, Satral, MS, India

[3] DSM's Arts, Commerce and Science College, Parbhani, Jintur, Maharashtra, 431509 India

[4] Department of Physics, Vivekanand College, Aurangabad, MS 431001 India

1 Introduction

Ferrimagnetic materials possess the combined properties of magnetic materials and insulators; this behavior is largely governed by the spin coupling of 3d electrons. Polycrystalline ferrites are very good dielectric materials, and very high dielectric constants are useful in designing good microwave devices such as isolators and switches [1, 2]. The dielectric properties of ferrites depend upon several factors including the method of preparation, chemical composition, grain structure or size, and amount and type of the additives [3]. Impedance spectroscopy is a suitable tool to study the electric and dielectric properties of materials. The conductivity material decreases with an increase in temperature (material metallic behavior) in the low-temperature region. At the high-temperature range, conductivity increases with an increase in temperature (semiconducting behavior).

Elastic properties of a solid are important because they relate to various fundamental solid-state properties such as interatomic potentials, equation of state, and phonon spectra. Elastic properties are also linked thermodynamically to the specific heat, thermal expansion, Debye temperature, melting point, and Gruneisen parameter. So, it is important to calculate elastic constants of solids. Infrared spectroscopy (IR) is the best characterization technique used (i) to study the various absorption bands in the spectrum; (ii) to determine the local symmetry in crystalline/noncrystalline solids, ordering phenomenon, and presence/absence of Jahn–Teller ions; and (iii) to determine force constants, elastic moduli, Debye temperature, and molar heat capacity [4]. IR spectra on the basis of different cations present on the A and B sites of the spinel lattice and force constant determination [5]; use of IR spectra to study other aspects of ferrite materials has not been explored in a systematic manner in depth.

Published online: 16 June 2016

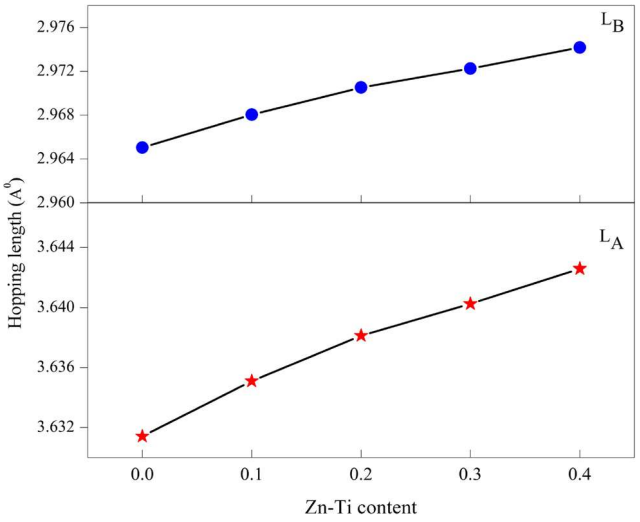

Fig. 1 Variation of hopping length for $CoZn_xTi_xFe_{2-2x}O_4$ spinel ferrites

It has been observed in literature that substitution of divalent Zn^{2+} and tetravalent Ti^{4+} nonmagnetic ions to replace Fe^{3+} in spinel ferrites results in an interesting crystal structure and electrical and magnetic properties. Shokrollahi et al. [6] have reported that the introduction of TiO_2 can improve the high-frequency loss properties of Mn–Zn cores. Electrical conductivity and complex electric modulus of titanium doped nickel–zinc ferrites for samples $Ni_{1+x-y}Zn_yTi_xFe_{2-2x}O_4$ [7]. The influence of Zn^{2+} and ion substitution on the resistivity and dielectric properties of $Ni_{0.65}Zn_{0.35+x}Fe_{1.99-2x}In_{0.01}Ti_xO_4$ ferrites has also been studied in the past [8]. This reveals that the substitution of coupled divalent Zn^{2+} and tetravalent Ti^{4+} metal ions influenced the properties of ferrites, and that motivated us to prepare Zn^{2+} and Ti^{4+} substituted $CoFe_2O_4$ with the chemical formula $CoZn_xTi_xFe_{2-2x}O_4$.

The aim of the present research paper is to study the effect of Ti and Zn ions on the IR spectroscopy and elastic and dielectric properties of the $CoZn_xTi_xFe_{2-2x}O_4$ (where $x = 0.0$ to $x = 0.4$) ferrite system. These studies may give valuable information on the elastic and dielectric properties, which are very important for practical application of $CoZn_xTi_xFe_{2-2x}O_4$ ferrites in the "ferrite core transformer."

2 Materials and Methods

The preparation of $CoZn_xTi_xFe_{2-2x}O_4$ nanoferrite samples has been reported in a previous work [9]. Infrared spectra were recorded in the wave number range 300–900 cm^{-1} using a Perkin-Elmer IR spectrometer. For recording IR spectra, powders were mixed with KBr in the ratio 1:300 by weight to ensure uniform dispersion in the KBr pellet. The mixed powders were then pressed in a cylindrical die to obtain a clear disc. The ultrasonic longitudinal (V_l) and shear (V_s) wave velocities of all the ferrite samples were determined by the ultrasonic pulse transmission method. In this method, 124.6 kHz PZT crystals and the calibrated range of an interferometer were used with an accuracy of error ± 5 m/s in velocity measurements. The dielectric constant (έ) and dielectric loss tangent (tan δ) were measured as a function of frequency at room temperature using an LCR-Q meter (Model Hioki 3532-50). The dielectric constant (έ) and loss tangent (tan δ) were calculated using the relation discussed in ref. [10].

3 Results and Discussion

3.1 Hopping and Bond Length

The distance between the magnetic ions, i.e., hopping length in the octahedral site (L_B) and the tetrahedral site (L_A), is calculated using the relation discussed elsewhere [11]. The variation of hopping lengths with Zn–Ti content x is shown Fig. 1. It is evident from Fig. 1 that hopping lengths L_A and L_B increased as the Zn–Ti content increases. This behavior of hopping lengths with Zn–Ti content x is attributed to the variation of the lattice constant with the Zn–Ti content x. Tetrahedral and octahedral bond lengths (d_{AX} and d_{BX}), tetrahedral edge, and shared and unshared octahedral edge (d_{AXE}, d_{BXE}, and d_{BXEU}) were calculated using the relation

Table 1 Oxygen parameter (U), lattice constant (a) (ref. [2]), tetrahedral d_{AX} and octahedral d_{BX} bond lengths, tetrahedral edge d_{AXE}, and shared d_{BXE} and unshared d_{BXEU} octahedral edge of the $CoZn_xTi_xFe_{2-2x}O_4$ system

Comp. (x)	Oxygen parameter U(Ǻ)	Lattice constant a(Ǻ)	d_{AX}(Ǻ)	d_{BX}(Ǻ)	Tetrahedral edge d_{AXE}(Ǻ)	Octahedral edge	
						d_{BXE}(Ǻ)	d_{BXEU}(Ǻ)
0.0	0.3837	8.3864	1.942	2.026	3.171	2.759	2.969
0.1	0.3849	8.3949	1.961	2.019	3.203	2.733	2.973
0.2	0.3861	8.4019	1.981	2.012	3.234	2.707	2.976
0.3	0.3874	8.4068	2.001	2.003	3.267	2.677	2.980
0.4	0.3886	8.4122	2.019	1.995	3.298	2.651	2.983

discussed elsewhere [11] and using the value of lattice constant 'a' and oxygen parameter 'u'. Values of these bond lengths are given in Table 1. Tetrahedral bond length d_{AX} and tetrahedral edge d_{AXE} both increased with the increase in Zn–Ti content x. This could be related to several facts such as a larger ionic radius of Zn–Ti ions as compared to that of Fe ions, variation in the lattice constant and oxygen parameter, and the fact that nonmagnetic Zn occupies strongly the tetrahedral A site [11, 12]. Octahedral bond lengths d_{BX} and octahedral shared d_{BXE} both decreased with the increase in Zn–Ti composition, and unshared octahedral edge d_{BXEU} does not vary much with composition.

3.2 IR Spectroscopy

IR spectroscopy has been used to investigate the various absorption bands in the prepared materials, and they have been analyzed on the basis of different cations present at the A and B sites of the spinel ferrites. The IR spectra exhibit three major IR vibration bands (Fig. 2); these bands have been rationalized on the basis of space group and symmetry both in normal and inverse spinel ferrites. According to Waldron [13], these IR vibration bands of the spinel ferrite are classified into two groups: high vibration band ν_1 appeared in the frequency range of 588–600 cm^{-1}, and low vibration band ν_2 appeared in the frequency range of 395–410 cm^{-1}. These bands are the common features of the spinel ferrite [13]. Appearance of ν_1 and ν_2 bands is expected due to the difference in the Fe^{3+}–O^{2-} distance for the A and B sites. The ν_3 band is observed in the range 330–337 cm^{-1}. Similar IR spectra have been observed in literature for rare earth element doped in Mg–Ti ferrites [14]. Values of the three vibrational bands (ν_1, ν_2, and ν_3) are present in Table 2. It is clear from Table 2 that the frequency of the band increased with the increasing Zn–Ti content. In the investigated ferrite system, Ti^{4+} occupied both the A and B sites by replacing Fe^{3+} ions which affects the band positions.

Table 2 Vibration frequency band position (ν) and force constant (K) of the $CoZn_xTi_xFe_{2-2x}O_4$ system

Comp. x	ν (cm^{-1}) [± 3]			K× 10^2 (N/m)	
	ν_1	ν_2	ν_3	K_t	K_o
0.0	588	395	331	1.479	0.950
0.1	590	398	333	1.537	0.959
0.2	592	400	334	1.583	0.962
0.3	594	405	335	1.630	0.980
0.4	598	409	337	1.689	0.992

Square brackets denote the estimated error

3.3 Force Constants and Debye Temperature

The force constant (K) is a second derivative of the potential energy with respect to internuclear separation. The force constants K_t and K_o are associated with the unit displacement of a cation-oxygen in the tetrahedral (A) and octahedral (B) sites, respectively. The force constant for the tetrahedral site (K_t) and octahedral site (K_o) is calculated using the relations discussed elsewhere [15]. The value of the force constant is included in Table 2, where it is observed that the force constants K_t and K_o both increased with the increase in Zn–Ti content x. This variation can be related to the difference in the ionic radii of Zn^{2+}, Ti^{4+}, and Fe^{3+} ions. The combined ionic radii of Zn^{2+} (0.82Å) and Ti^{4+} (0.60Å) ions are greater than those of Fe^{3+} ions (0.67Å).

The Debye temperature (θ_I) of all the samples is obtained using the following relation:

$$\theta_I = \frac{hC\nu_{av}}{k} \tag{1}$$

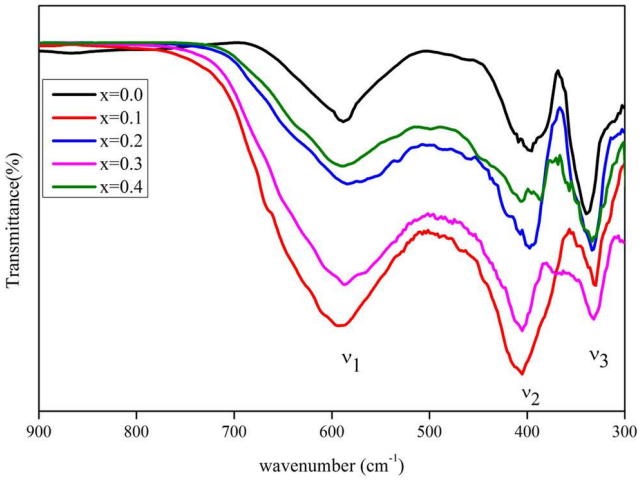

Fig. 2 IR spectra of $CoZn_xTi_xFe_{2-2x}O_4$ at room temperature

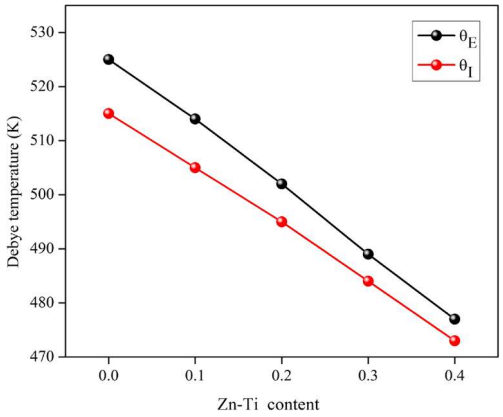

Fig. 3 Variation of Debye temperature for $CoZn_xTi_xFe_{2-2x}O_4$ spinel ferrites

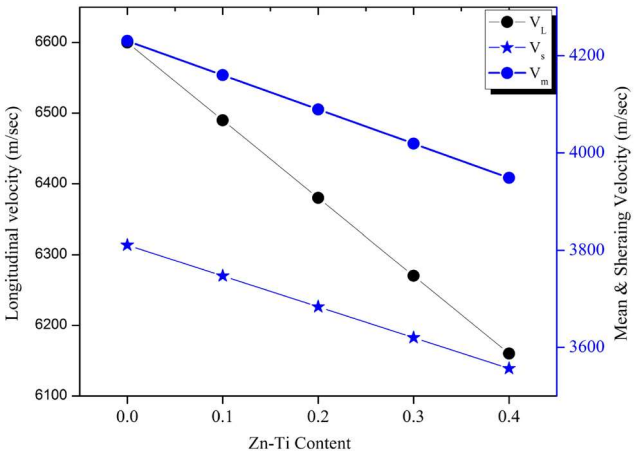

Fig. 4 Variation of wave velocity for $CoZn_xTi_xFe_{2-2x}O_4$ at room temperature

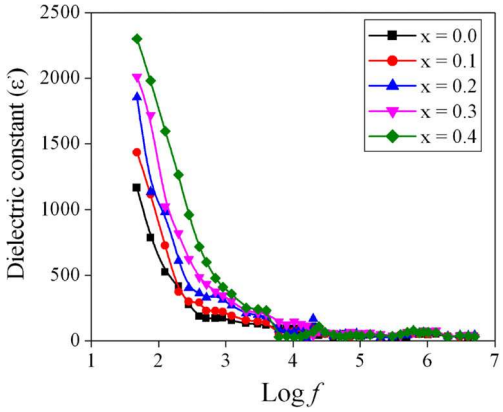

Fig. 6 Variation of dielectric constant with frequency for $CoZn_xTi_xFe_{2-2x}O_4$ at room temperature

where k is the Boltzmann constant, C is the velocity of light ($C = 3 \times 10^8$ cm/s), and ν_{av} is the average wave number of bands. The variation of the Debye temperature with the Zn–Ti content is shown in Fig. 3. It is observed from Fig. 3 that the Debye temperature decreased with the increase in Zn–Ti composition. This behavior of the Debye temperature is related to the wave number of vibrational bands of IR spectra.

3.4 Elastic Constant, Poisson Ratio, and Debye Temperature

Ultrasonic wave velocity such as longitudinal (V_l) and shear (V_s) wave velocities was measured by using the ultrasonic pulse transmission method at room temperature. The values of the two velocities V_l and V_s were used to calculate the mean velocity (V_m) [16]. The values of these obtained velocities are represented in Fig. 4. It can be seen from Fig. 4 that V_l, V_s and V_m were decreased with the increase in Zn–Ti ions. Similar behavior is observed in Zn-doped LiMg and LiMgTi ferrites [17]. It is seen from Fig. 4 that the values of shear wave velocity are less than those of longitudinal wave velocity. This is because when a wave travels through a material, due to transfer of energy, it makes the particles vibrate and collide with each other which causes other particles to vibrate. In the case of shear waves, a particle in a medium vibrates transversely to the direction of propagation of wave motion, and hence, it requires a larger energy to make the neighboring particles vibrate [18].

Longitudinal modulus (L), Young's modulus (E), rigidity modulus (G), bulk modulus (K), and Poisson's ratio (s) have been calculated using the relation discussed elsewhere [19], and their variation is shown in Fig. 5. Figure 5 shows that all elastic moduli decreased with the increase in Zn–Ti content x. This behavior of elastic moduli is attributed to interatomic binding between various atoms in spinel ferrites. In cobalt's ferrites, interatomic bonding between Zn–Fe and Ti–Fe ions decreased. The values of Poisson's

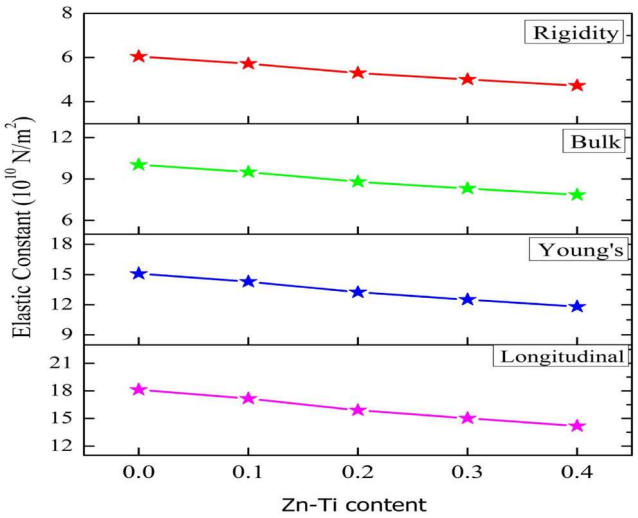

Fig. 5 Variation of elastic moduli for $CoZn_xTi_xFe_{2-2x}O_4$ at room temperature

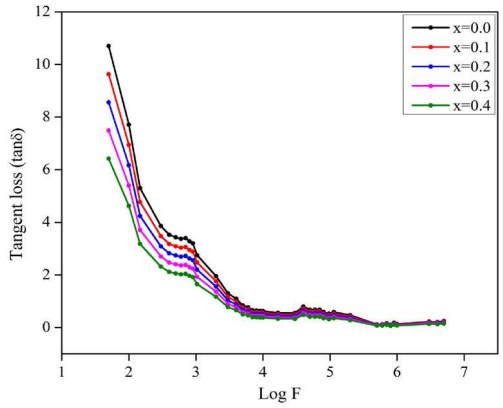

Fig. 7 Variation of dielectric loss tangent with frequency for $CoZn_xTi_xFe_{2-2x}O_4$ at room temperature

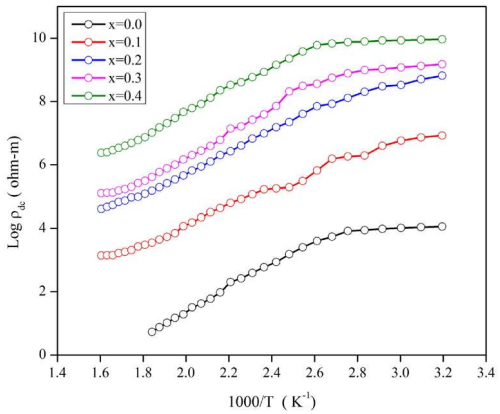

Fig. 8 Variation of dc electrical resistivity with temperature for $CoZn_xTi_xFe_{2-2x}O_4$ spinel ferrites

ratio for all the samples almost remain constant. The value is 0.25; this value of the Poisson ratio is in good agreement with the $Li_{0.35}Mg_{0.3}Zn_{0.2}Ti_{0.2}Mn_{0.1}Fe_{1.85}O_4$ ferrite system [17].

The acoustic Debye temperature (θ_E) provides useful information for thermal properties and elastic properties in particular. As such, the acoustic Debye temperature has also been calculated for all the samples using the Anderson formula [19, 20]. The variation of the acoustic Debye temperature with Zn–Ti content is shown in Fig. 3. It is seen from Fig. 3 that the acoustic Debye temperature decreased with the increase in Zn–Ti composition. It is clear that the behavior of the acoustic Debye temperature is dependent on the variation of the wave velocity and bulk density of samples. The Debye temperatures (θ_I) calculated through IR data and the Debye temperature (θ_E) calculated by wave velocity are in good agreement with each other.

3.5 Dielectric Constant

The variation of the dielectric constant (ε') at room temperature in the frequency range 50 Hz to 5 MHz is shown in Fig. 6. It can be observed from Fig. 6 that the dielectric constant decreased with increasing frequency from 50 Hz to 1 kHz. The dielectric dispersion has been explained in the light of Maxwell Wagner interfacial polarization in accordance with the Koop phenomenological theory. The increase of the dielectric constant with Zn and Ti substitution in cobalt ferrite is observed in Fig. 6, which is basically related to the higher dielectric constant of Ti^{4+}. The similar nature of the dielectric constant is reported for Zn- and Ti-doped lithium ferrites [21]. Figure 7 shows the variation of the dielectric loss tangent (tan δ) with frequency at room temperature. It is observed that the dielectric loss tangent decreased with an increase in frequency.

3.6 dc Resistivity

The dc resistivity was measured using the two-probe method in the temperature range of 300–600 K. Figure 8 shows the variation of dc resistivity with temperature for all the samples under investigation. It can be seen that the dc electrical resistivity decreased with an increase in temperature, which indicates that all samples possess semiconducting behavior. Further, the dc resistivity increased with an increase in Zn–Ti ions. Figure 8 shows the two regions with different slopes; the break of curve in dc resistivity indicates that difference in electrical conduction with temperature that corresponds to the transition point that refers to Curie temperature (Tc). The Curie temperature determined from the dc resistivity graph is included in Table 3. A decrease in Tc with the increase in Zn–Ti content x is observed in Table 3. This decrease in Tc can be explained on the basis of the number of magnetic ions present in two sub-lattices in spinel ferrites. The conduction mechanism in a semiconductor is usually explained on the basis of hopping mechanism due to space charge. The electron exchange between Fe^{3+} and Fe^{2+} and hole transfer Ti^{3+} and Ti^{4+} on the octahedral B site in ferrites are according to the Varwey mechanism [22]. The hole and electron exchange on the octahedral B site are as follows [23].

$$Fe^{2+} \leftrightarrow Fe^{3+} + e$$
$$Ti^{3+} \leftrightarrow Ti^{4+} + e^{-}$$
$$Co^{3+} \leftrightarrow Co^{2+} + e \text{ (hole)}$$

Table 3 Activation energies (E_P, E_f and Δ E) and Curie temperature (T_C) of the $CoZn_xTi_xFe_{2-2x}O_4$ ferrite system

Comp. x	Activation energies (eV) [± 0.001]			Curie temperature T_C (K)
	E_p	E_f	ΔE	
0.0	0.236	0.100	0.136	600
0.1	0.260	0.112	0.148	580
0.2	0.276	0.124	0.152	565
0.3	0.291	0.130	0.161	546
0.4	0.306	0.134	0.172	530

The value in square brackets indicates the estimated error

The Fe^{2+}, Ti^{3+}, and Co^{3+} ions formed during the annealed process [24]. The activation energies were calculated using the Arrhenius relation:

$$\rho_{\mathrm{dc}} = \rho_o e^{\frac{\Delta E_g}{kT}} \quad (2)$$

Values of activation energies are listed in Table 3. It is observed that the activation energies increased with Zn and Ti composition. The increase in activation energies is due to the increase in hopping lengths of the octahedral B site.

4 Conclusions

The results of this investigation can be summarized as follows:

- Hopping length and tetrahedral bond length increased with Zn–Ti ion substitution increase.
- Three absorption bands were observed in IR spectra confirming the spinel structure of prepared samples.
- The force constant of two sites increased with the increase in Zn–Ti ion substitution in cobalt ferrite.
- The elastic moduli of all samples decreased with the increase in Zn–Ti composition.
- Debye temperature determined from IR spectra and elastic data are in good agreement with each other.
- The dc resistivity and dielectric constant increased whereas the dielectric loss tangent of $CoFe_2O_4$ decreased with Zn–Ti substitution. This may be of technological importance as this material can be applicable in the "ferrite core transformer."

Compliance with Ethical Standards

Conflict of interests The authors declare that they have no conflict of interest.

References

1. Mujasam Batoo, K., Kumar, S., Lee, C.G.: Alimuddin, Study of dielectric and ac impedance properties of Ti doped Mn ferrites. Curr. Appl. Phys. **9**, 1397–1406 (2009)
2. Ravinder, D., Reddy, P.V.B., Frequency, P.S.: composition dependence of dielectric behavior of copper substituted lithium ferrites. J. Mater. Sci. Lett. **22**, 1599 (2003)
3. Xiao, H.M., Liu, X.M., Synthesis, S.Y.Fu.: magnetic and microwave absorbing properties of core-shell structured $MnFe_2O_4/TiO_2$ nanocomposites. Comp. Sci. Tech. **66**, 2003 (2006)
4. Patange, S.M., Shirsath, S.E., Jadhav, S.P., Hegade, V.S., Kamble, S.R., Jadhav, K.M.: Elastic properties of nanocrystalline aluminum substituted nickel ferrites prepared by co-precipitation method. J. Mol. Struct. **1038**, 40 (2013)
5. Hashim, M., Alimuddin, S.K., Shirsath, S.E., Kotnala, R.K., Shah, J.: Ravi Kumar. Influence of Cr^{3+} ion on the structural, ac conductivity and magnetic properties of nanocrystalline Ni–Mg ferrite. Ceram. Int. **39**, 1807 (2013)
6. Shokrollahi, H., Janghorban, K.: Influence of additives on the magnetic properties, microstructure and densification of Mn–Zn soft ferrites. J. Mater. Sci. Eng. B **141**, 91 (2007)
7. Kaiser, M.: Electrical conductivity and complex electric modulus of titanium doped nickel–zinc ferrites. Physica B **407**, 606–613 (2012)
8. Rao, B.P., Rao, K.H., Rao, T.V., Paduraru, A.: Pulsed laser deposition of Ni-Zn ferrite thin films, O.F. Caltun. J. Opt. Adv. Mater. **7**, 701 (2005)
9. Patange, S.M., Desai, S.S., Meena, S.S., Yusuf, S.M., Sagar, E.: Shirsath. Random site occupancy induced disordered Néel-type collinear spin alignment in heterovalent Zn^{2+}–Ti^{4+}ion substituted $CoFe_2O_4$. RSC Adv **5**, 91482 (2015)
10. Gul, I.H., Ahmed, A., Maqsood, A.: Electrical and magnetic characterization of nanocrystalline Ni–Zn ferrite synthesis by co-precipitation route. J. Magn. Magn. Mater **320**, 270 (2008)
11. Jadhav, S.S., Shirsath, S.E., Tokshay, B.G., Patange, S.M., Shukla, S.J., Jadhav Intern, K.M.: Structural properties and cation distribution of Co-Zn nano-ferrites. J. Mod. Phys. B **23**, 5629 (2009)
12. Amer, M.A., Hitti, M.E.: Mössbauer and X-ray studies for $Ni_{0.2}Zn_xMg_{0.8-x}Fe_2O_4$ ferrites. J. Magn. Magn. Mater. **234**, 118–125 (2001)
13. Waldron, R.D.: Infrared spectra of ferrites. Phys. Rev. B **99**, 1727 (1955)
14. Ahmed, M.A., Ateia, E., Salem, F.M.: Spectroscopic and electrical properties of Mg–Ti ferrite doped with different rare-earth elements. Physica B **381**, 144–155 (2006)
15. Patange, S.M., Shirsath, S.E., Jadhav, S.P., Hogade, V.S., Kamble, S.R., Jadhav, K.M.: Elastic properties of nanocrystalline aluminum substituted nickel ferrites prepared by co-precipitation method. J. Mole. Struct. **1038**, 40–44 (2013)
16. Abu-Elsaad, N.I.: Elastic properties of germanium substituted lithium ferrite. J. Mole. Struct. **1075**, 546–550 (2014)
17. Kumar, N., Purushotham, Y., Venugopal Reddy, P., Zaidi, Z.H., Kishan, P.: Elastic behaviour of Zn-substituted LiMg and LiMgTi ferrites. J. Magn. Magn. Mater. **192**, 116–120 (1999)
18. Shirsath, S.E., Patange, S.M., Kadam, R.H., Mane, M.L., refinement, K.M.Jadhav.S.tructure., location, c.ation.s.ite.: spectral and elastic properties of Zn^{2+} substituted $NiFe_2O_4$. J. Mole. Struct. **1024**, 77–83 (2012)
19. Algude, S.G., Patange, S.M., Sagar, E., Shirsath, D.R., Mane, K.M.: Jadhav. Elastic behaviour of Cr^{3+} substituted Co-Zn ferrites. J. Magn. Magn. Mater. **350**, 39–41 (2014)
20. Anderson, O.L.: A simplified method for calculating the Debye temperature from elastic constants. J. Phys. Chem. Solids **24**, 909 (1963)
21. Verma, V., Pandey, V., Shukla, V.N., Annapoorni, S., Kotnala, R.K.: Remarkable influence on the dielectric and magnetic properties of lithium ferrite by Ti and Zn substitution. Solid State Commun. **149**, 1726–1730 (2009)
22. Verwey, E.J.W., de Boer, J.H.: Cation arrangement in a few oxides with crystal structures of the spinel type. Red. Trav. Chim. Phys. Bas. **55**, 531–540 (1936)
23. Eraky, M.R., Attia, S.M.: Transport properties of Ti–Ni spinel ferrites. Physica B **462**, 97–103 (2015)
24. Lotgering, F.K., Semiconduction and cation valencies in manganese ferrites: J. Phys. Chem. Solids **25**, 95–103 (1964)